Experimental and Computational Evidence for an Inversion in Guest Capacity in High-Generation Triazine Dendrimer Hosts

Jongdoo Lim,[†] Giovanni M. Pavan,[‡] Onofrio Annunziata,[†] and Eric E. Simanek*,[†]

[†]Department of Chemistry, Texas Christian University, Fort Worth, Texas 76129, United States
[‡]Laboratory of Applied Mathematics and Physics (LamFI), University for Applied Sciences of Southern Switzerland (SUPSI), Centro Galleria 2, CH-6928 Manno, Switzerland

S *Supporting Information*

ABSTRACT: The synthesis, characterization, and host–guest chemistry of high-generation triazine dendrimers are described. With pyrene and camptothecin as guests, experiments revealed that the guest capacity of odd-generation triazine dendrimers increased until generation 7 but decreased at generation 9. Molecular dynamics simulations conducted in explicit solvent showed a useful fingerprint for this behavior in radial distribution functions of water molecules penetrating the interior of the dendrimers. A linear relationship between the guest capacity of dendrimers measured experimentally and the number of water molecules within the interior determined computationally was observed.

Since its inception, the field of dendrimer science has been intertwined with those of supramolecular chemistry and molecular recognition.[1] As each new class of dendrimers has appeared, studies of host–guest potential have soon followed. Host–guest chemistry offers inroads into many problems, perhaps most notably drug delivery. Seminal studies have punctuated and inspired the field, including Meijer's dendritic box.[2] General trends have emerged, including the relationship between the size of the dendrimer host and its capacity to harbor hydrophobic guests.[3] This correlation is derived primarily from evidence using low-generation dendrimers. For low-generation triazine dendrimers, this trend has been observed.[4] However, exceptions to this trend have been noted. For example, Crooks and co-workers[5] observed a decreased catalytic rate in hydrogenation of small olefins with increasing generation (G4, G6, and G8) of poly(amidoamine) (PAMAM) dendrimers containing Pd nanoparticles. They attributed this behavior to limited accessibility of the substrates to the interior of the dendrimer. Lopina and co-workers[6] observed that the solubilization of pyrene in water by G3 PAMAM was reduced when longer poly(ethylene glycol) (PEG) (5 kDa) arms were substituted for shorter PEG (2 kDa) arms.

Herein, the synthesis of high-generation triazine dendrimers and an inversion of their guest capacity are described. Only a handful of high-generation dendrimers are available. Among these, Tomalia's PAMAM dendrimers[7] can be synthesized on a large scale via a divergent route and are commercially available up to generation 10. Meijer's poly(propyleneimine) (PPI) dendrimers[8] can be synthesized on a multikilogram scale up to

at least generation 5. The phosphorus-based dendrimers pioneered by Majoral and Caminade[9] can be synthesized up to generation 12 and are commercially available for two subtypes, thiophosphoryl dendrimers (up to G10) and cyclotriphosphazene dendrimers (up to G6).

We report that through a macromonomer route, triazine dendrimers can be prepared up to generation 11, whereat the poor aqueous solubility of the cationic dendrimers preclude further iteration. The synthesis is accomplished using a divergent, iterative reaction cycle wherein two generations are added with every two steps: addition of a monochlorotriazine macromonomer and deprotection (Chart 1).

Chart 1. Synthesis of High-Generation Triazine Dendrimers: (top) Structures of the Core and Repeating Unit; (bottom) General Scheme
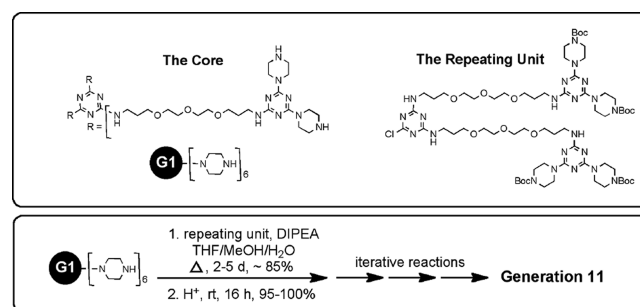
The use of a monochlorotriazine macromonomer has the advantage of precluding covalent cross-linking of dendrimers during synthesis: It has a single reactive site. In contrast, PAMAM synthesis employs reaction with ethylenediamine thus affording this unfavorable possibility. The use of a flexible, hydrophilic polyether linker here, instead of the aliphatic linkers explored previously,[10] improves the solubility of these dendrimers. The targets and selected data appear in Table 1.

Dendrimers present a challenge to characterization. Data can be derived from multiple sources. ^{1}H NMR spectroscopy showed the oscillating appearance and disappearance of characteristic peaks derived from the peripheral piperazines. Such data has inherent limitations in regard to signal-to-noise ratio (Figure 1).

Table 1. Summary for G3−G11 Dendrimers

	G3	G5	G7	G9	G11
Ends[a]	24 (24)	96 (92+)	384 (360+)	1536 (NA)	6144 (NA)
MW[b] (calcd)	7539	31785	128800	516700	2068500
MW[c] (obsd)	7521	31764	123k-129k	NA	NA
$R^{h\,d}$ (nm)	2.81	3.14	5.24	8.99	N.A.
$R^{g\,e}$ (nm)	2.0	2.4	4.1	7.3	9.0
Pyr[f]	0.08	0.16	0.25	0.19	N.A.
CPT[f]	1.5	3.7	8.3	6.3	N.A.

[a]Theoretical number of surface groups; the number observed by mass spectrometry is given in parentheses. [b]Theoretical molecular weight in daltons. [c]Observed molecular weight in daltons. G3 was a single species, G5 showed a trace side product resulting from incomplete reaction, and G7 showed a broad signal with a width of 6 kDa. [d]Hydrodynamic radius determined from DLS in PBS at 25 °C using the Stokes−Einstein equation. [e]Radius of gyration obtained from MD simulations. [f]Number of pyrene (Pyr) or camptothecin (CPT) molecules solubilized per molecule of dendrimer, as determined experimentally by an extraction protocol.
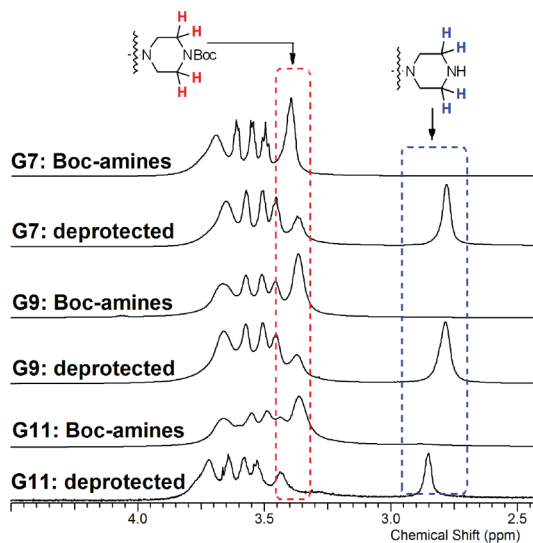

Figure 1. ^{1}H NMR spectra of the high-generation dendrimers in the expanded region from 4.5 to 2.5 ppm (500 MHz, CDCl$_3$). The vicinal proton (blue) signals of the free amines on the peripheral piperazines appear in the blue dashed line box, whereas the vicinal proton (red) signals of the Boc-protected amines on the peripheral piperazines appear in the red dashed line box, overlapping the signals of −NHCH$_2$CH$_2$CH$_2$O−.

MALDI-TOF mass spectrometry has proven useful for low- and moderate-generation triazine dendrimers with molecular weights up to ∼100 kDa. The spectrum of the G3 target shows a single species. The trace for G5 shows evidence of a minor product resulting from failure to incorporate a single macro-monomer of the 24 appended. This leads to products with either 92 or 96 end groups. The mass ion of the hydrophobic

Boc-protected G7 dendrimer was not observed. However, upon deprotection of G7 (and a 40 kDa reduction in mass), the amine-terminated G7 dendrimer showed a broad peak from 123 to 129 kDa. We interpret this trace as being indicative of a mixture of products that are missing up to six macromonomers.

Mass spectrometry failed to give molecular weight information for the higher-generation dendrimers G9 and G11. We would predict the number of failed reactions to increase over the course of the synthesis, leading to greater dispersity in the products assigned to G9 and G11. Evidence for synthetic success for these two species was derived from other sources, including NMR, dynamic light scattering (DLS), and changes in physical properties. The extent to which G9 and G11 reflect the idealized structure, however, is largely unknown.

DLS revealed increasing size [i.e., hydrodynamic radius (R_h)] with increasing generation (Table 1). The trend in the R_h data corroborated the sizes [i.e., radii of gyration (R_g)] determined by molecular dynamics (MD) simulations. DLS also provided evidence for the onset of the globular dendrimer structure. A plot of $\log(R_h)$ versus $\log(MW)$ showed an exponent of 0.377 for the deprotected G5, G7, and G9 dendrimers. An exponent of 0.333 corresponds to a homogeneous sphere or a compact coil in a bad solvent, while an exponent of 0.500 corresponds to an ideal random coil.[11] The value for G3 displayed a positive deviation that can be attributed to a more elongated shape in comparison with the other larger dendrimers.

Guest capacity was measured using an extraction protocol. An interesting deviation from the expected correlation of increasing guest capacity with increasing generation was observed when the ability of these dendrimers to serve as hosts was assessed using the small, hydrophobic guests pyrene and camptothecin. The number of guests per dendrimer increased until generation 7 but decreased unexpectedly at generation 9. These data are reported in Table 1 as the average of five replicates. Within both the camptothecin and pyrene series, all of the values reported for the various generations are statistically different.

MD simulations with explicit water molecules and ions from NaCl (150 mM) offer insight into this behavior. Table 1 shows snapshots from these simulations. Enlarged pictures appear in the Supporting Information. Through generation 7, the dendrimers are porous and flexible. Surface crowding becomes significant at G9.

This behavior is reflected in the calculated radial distribution functions (RDFs).[12] These plots report the distributions of atoms with respect to the center of mass of the dendrimer over the MD trajectories (Figure 2). The RDFs for the smaller-generation (G3−G7) dendrimers show high peaks near the core and low densities at the surface, indicating that they are
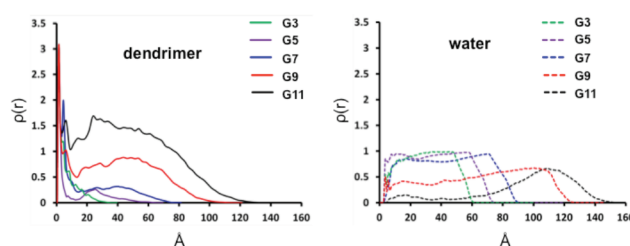

Figure 2. RDFs for the dendrimers (left) and molecules of water (right).

flexible in water. Molecules of water penetrate close to the core of the dendrimer. The situation changes for the larger-generation dendrimers. The surface of G9 is saturated and dense, resulting in a loss of flexibility and back-folding. Crowding is so severe in G11 that water penetration is limited. This onset of steric crowding occurring around generation 9 for these triazine dendrimers was also observed for PAMAM dendrimers at similar generations (G8−10).[13] The RDFs calculated for water molecules (Figure 2) reinforce this picture.

The host−guest capacity can be rationalized and predicted using computation by counting the number of water molecules within the dendrimers.[14] Figure 3 plots the experimentally
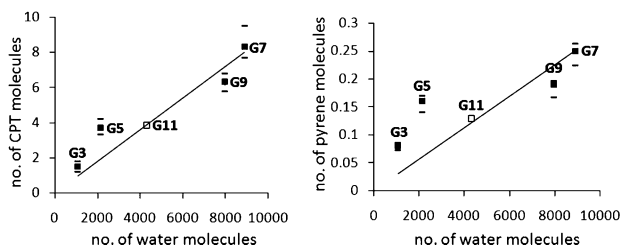

Figure 3. Plots of guest capacity per dendrimer against the number of water molecules within the interior of the dendrimer (data for G3−G9 are shown as filled squares) for (left) camptothecin (CPT) and (right) pyrene. The correlation was arbitrarily extrapolated to zero. The predicted guest capacity for G11 is shown as an open square. The standard deviations of individual points are not shown because the values are smaller than the symbols. Instead, the range of five values determined experimentally is indicated with bars.

determined guest capacity against the computationally determined number of water molecules within the interior of the dendrimer. Here, a diminished guest capacity at G9 was predicted and observed. Moreover, the capacity of G11 (open square) was predicted to be similar to that of G5 and much smaller than that of G7. Limited solubility prevented experimental studies of G11. The bars shown reflect the range of reported values for five replicates.

In conclusion, triazine dendrimers join a select group of materials available at large generations. The inversion of the guest capacity observed for these high-generation dendrimer hosts is consistent with the results obtained from MD simulations. Typically, the guest capacity increases as function of generation in low-generation materials. This observation may derive from the limited number of high-generation dendrimers assessed or from some peculiarity (e.g., hydrophobicity, back-folding) associated with the system chosen.[15]

Simulations provide a useful fingerprint for predicting host−guest capacity. Removing the burden of synthesis and relying on computation, open opportunities for facilitated design in silico, particularly in terms of the choice of linking groups incorporated during dendrimer synthesis.

The guest capacity is related to the structure of the guest: camptothecin and pyrene show 20-fold differences in encapsulation. Such differences in capacity are not surprising, as the equilibrium position is expected to be a function of the guest, dendrimer, and solvent.[15] Whether this compositional dependence on the capacity represents an opportunity for tuning the host or guest composition for a specific application is unknown. However, the current low guest capacity of these dendrimers underscores the value of covalent strategies in applications such as drug delivery.

■ ASSOCIATED CONTENT

⑤ Supporting Information

Details of synthesis, characterization, computation, analysis, and statistical treatment. This material is available free of charge via the Internet at http://pubs.acs.org.

■ AUTHOR INFORMATION

Corresponding Author

e.simanek@tcu.edu

■ ACKNOWLEDGMENTS

■ REFERENCES

(1) (a) Percec, V.; Peterca, M.; Dulcey, A. E.; Imam, M. R.; Hudson, S. D.; Nummelin, S.; Adelman, P.; Heiney, P. A. *J. Am. Chem. Soc.* **2008**, *130*, 13079. (b) Percec, V.; Dulcey, A. E.; Balagurusamy, V. S.; Miura, Y.; Smidrkal, J.; Peterca, M.; Nummelin, S.; Edlund, U.; Hudson, S. D.; Heiney, P. A.; Duan, H.; Magonov, S. N.; Vinogradov, S. A. *Nature* **2004**, *430*, 764. (c) Zeng, F.; Zimmerman, S. C. *Chem. Rev.* **1997**, *97*, 1681. (d) Gillies, E. R.; Fréchet, J. M. J. *Drug Discovery Today* **2005**, *10*, 35. (e) Medina, S. H.; El-Sayed, M. E. *Chem. Rev.* **2009**, *109*, 3141. (f) Scott, R. W.; Datye, A. K.; Crooks, R. M. *J. Am. Chem. Soc.* **2003**, *125*, 3708. (g) Twyman, L. J.; King, A. S.; Martin, I. K. *Chem. Soc. Rev.* **2002**, *31*, 69. (h) Kaanumalle, L. S.; Nithyanandhan, J.; Pattabiraman, M.; Jayaraman, N.; Ramanurthy, V. *J. Am. Chem. Soc.* **2004**, *126*, 8999. (i) Kwon, T.-H.; Kim, M. K.; Kim, M. K.; Kwon, J.; Shin, D.-Y.; Park, S. J.; Lee, C.-L.; Kim, J.-J.; Hong, J.-I. *Chem. Mater.* **2007**, *19*, 3673. (j) Villaraza, A. J.; Bumb, A.; Brechbiel, M. W. *Chem. Rev.* **2010**, *110*, 2921. (k) Astruc, D.; Boisselier, E.; Ornelas, C. *Chem. Rev.* **2010**, *110*, 1857.

(2) (a) Jansen, J. F. G. A.; de Brabander-van den Berg, E. M. M.; Meijer, E. W. *Science* **1994**, *266*, 1226. (b) Versteegen, R. M.; van Beek, D. J.; Sijbesma, R. P.; Vlassopoulos, D.; Fytas, G.; Meijer, E. W. *J. Am. Chem. Soc.* **2005**, *127*, 13862.

(3) (a) Kline, K. K.; Morgan, E. J.; Norton, L. K.; Tucker, S. A. *Talanta* **2009**, *78*, 1489. (b) Kojima, C.; Kono, K.; Maruyama, K.; Takagishi, T. *Bioconjugate Chem.* **2000**, *11*, 910.

(4) (a) Zhang, W.; Lalwani, S.; Chouai, A.; Simanek, E. E. *Isr. J. Chem.* **2009**, *49*, 23. (b) Zhang, W.; Jiang, J.; Qin, C.; Pérez, L. M.; Parrish, A. R.; Safe, S. H.; Simanek, E. E. *Supramol. Chem.* **2003**, *15*, 607.

(5) Niu, Y.; Yeung, L. K.; Crooks, R. M. *J. Am. Chem. Soc.* **2001**, *123*, 6840.

(6) Yang, H.; Morris, J. J.; Lopina, S. T. *J. Colloid Interface Sci.* **2004**, *273*, 148.

(7) (a) Tomalia, D. A.; Baker, H.; Dewald, J. R.; Hall, M.; Kallos, G.; Martin, S.; Roeck, J.; Ryder, J.; Smith, P. *Polym. J.* **1985**, *17*, 117. (b) Tomalia, D. A.; Naylor, A. M.; Goddard, W. A. III. *Angew. Chem., Int. Ed. Engl.* **1990**, *29*, 138.

(8) Bosman, A. W.; Janssen, H. M.; Meijer, E. W. *Chem. Rev.* **1999**, *99*, 1665.

(9) (a) Majoral, J.-P.; Caminade, A.-M. *Top. Curr. Chem.* **1998**, *197*, 79. (b) Slaney, M.; Bardaji, M.; Casanove, M.-J.; Caminade, A.-M.; Majoral, J.-P.; Chaudret, B. *J. Am. Chem. Soc.* **1995**, *117*, 9764.

(10) (a) Lim, J.; Mintzer, M. A.; Perez, L. M.; Simanek, E. E. *Org. Lett.* **2010**, *12*, 1148. (b) Crampton, H.; Hollink, E.; Perez, L. M.; Simanek, E. E. *New J. Chem.* **2007**, *31*, 1283.

(11) Schmidt, K. S. *Introduction to Dynamic Light Scattering by Macromolecules*; Academic Press: San Diego, 1990; p 292.

(12) (a) Shema-Mizrachi, M.; Pavan, G. M.; Levin, E.; Danani, A.; Lemchoff, N. G. *J. Am. Chem. Soc.* **2011**, *133*, 14359. (b) Pavan, G. M.; Kostiainen, M. A.; Danani, A. *J. Phys. Chem. B* **2010**, *114*, 5686.

(13) (a) *Handbook of Nanoscience, Engineering, and Technology*, 2nd ed.; Goddard, W. A., III, Brenner, D. W., Lyshevski, S. E., Iafrate, G. J.,

Eds.; CRC Press: Boca Raton, FL, 2007. (b) Maiti, P. K.; Çağin, T.; Wang, G.; Goddard, W. A. III. *Macromolecules* **2004**, *37*, 6236. (c) de Gennes, P. G.; Hervet, H. J. *J. Phys., Lett.* **1983**, *44*, 351.

(14) These values were determined by assigning the interior as a sphere with a radius equal to the R_g value calculated from MD simulations.

(15) (a) Aulenta, F.; Hayes, W.; Rannard, S. *Eur. Polym. J.* **2003**, *39*, 1741. (b) Boas, U.; Heegaard, P. M. H. *Chem. Soc. Rev.* **2004**, *33*, 43. (c) Zimmerman, S. C.; Lawless, L. J. *Top. Curr. Chem.* **2001**, *217*, 95.